EUROPEAN JOURNAL OF PURE AND APPLIED MATHEMATICS
2025, Vol. 18, Issue 3, Article Number 6149
ISSN 1307-5543 – ejpam.com
Published by New York Business Global

A Mathematical Model for COVID-19 and Tuberculosis Co-infection with the Effect of Quarantine Measure

Julito A. Puebla Jr[1,*], Jay Michael R. Macalalag[2], Kaye Y. Pajaron[2]

[1] *Department of General Education, Caraga State University Cabadbaran Campus, 8605 Cabadbaran City, Philippines*
[2] *Department of Mathematics, Caraga State University, 8600 Butuan City, Philippines*

Abstract. In this paper, a deterministic mathematical model for the transmission dynamics of COVID-19 and tuberculosis co-infection, using a system of nonlinear ordinary differential equations, is proposed and analyzed. We begin our mathematical analysis of the COVID-19 and tuberculosis sub-models by establishing the existence, uniqueness, non-negativity, and boundedness of the solutions. Subsequently, we determine the equilibrium points and the reproduction numbers of the sub-models as well as the co-infection model. We then proceed to prove that the disease-free equilibrium point of each sub-model and the co-infection model is locally and globally asymptotically stable if its corresponding reproduction number is less than 1 and unstable otherwise. Moreover, if the reproduction number is greater than 1, then the corresponding sub-model is locally asymptotically stable at the endemic equilibrium point. Numerical simulations are conducted to validate the theoretical findings. This study demonstrates that effective quarantine measures are crucial for controlling and potentially eradicating COVID-19 and tuberculosis co-infections.

2020 Mathematics Subject Classifications: 92D30, 34D23, 92C60, 34C60, 37N25

Key Words and Phrases: COVID-19, tuberculosis, coinfection, stability analysis, reproduction number

1. Introduction

Infectious diseases, caused by pathogenic microorganisms, invade the body and disrupt normal functions. They can be transmitted through direct contact, contaminated surfaces, or vectors. These diseases range from mild to life-threatening, affecting various organs and systems. Throughout history, they have shaped societies, caused epidemics, and influenced human history. Coronavirus disease (COVID-19) and tuberculosis (TB) exemplify the immense suffering, loss of life, and social disruptions caused by infectious diseases that persist worldwide [45].

*Corresponding author.
DOI: https://doi.org/10.29020/nybg.ejpam.v18i3.6149

Email addresses: julito.puebla@csucc.edu.ph (J. Puebla),
jrmacalalag@carsu.edu.ph (JM. Macalalag), kayepajaron@gmail.com (K. Pajaron)

The COVID-19 pandemic is a global health crisis caused by the severe acute respiratory syndrome coronavirus 2 (SARS-CoV-2) [20]. It was first identified in December 2019 in Wuhan, Hubei Province, China. On March 11, 2020, the virus quickly spread to other parts of China and subsequently to numerous countries around the world, leading to the declaration of a pandemic by the World Health Organization (WHO). The virus spreads primarily through droplets when an infected person talks, coughs, or sneezes, and can also spread by touching a contaminated surface and then touching one's mouth, nose, or eyes [8]. In January 2025, there have been 777,349,085 confirmed cases of COVID-19 infection, with 7,086,633 confirmed deaths in the whole country [38]. In the Philippines, in January 2025 there were 4,140,383 confirmed cases of COVID-19 with 66,864 deaths reported to the WHO [30]. This indicates that COVID-19 continues to pose significant global challenges in terms of public health and economic impact.

On the other hand, tuberculosis (TB) is a contagious respiratory infectious disease caused by the *Mycobacterium tuberculosis*. It affects primarily the lungs, but can also target other parts of the body such as the kidneys, spine, and brain. Tuberculosis spreads through the air when an infected individual coughs, sneezes, or talks, releasing tiny droplets containing the bacteria [36]. In total, approximately 10.6 million people fell ill with tuberculosis and 1.6 million people died of tuberculosis in 2021 [39]. Eight countries with the highest number of new tuberculosis infections in 2023 are India (26%), China (8.5%) Indonesia (8.4%), Philippines (6.0%), Pakistan (5.8%), Nigeria (4.6%), Bangladesh (3.6%), and South Africa (3.6%) [41]. This indicates that tuberculosis is one of the major global health concerns in these countries, particularly in the Philippines.

COVID-19 and tuberculosis are both infectious diseases primarily transmitted through close contact. Co-infection occurs when an individual is simultaneously infected with COVID-19 and tuberculosis. Co-infected individuals experience similar symptoms such as cough, fever, and difficulty breathing. The study reported in [9] has confirmed that latent and active TB are the primary risk factors for increasing the transmission of COVID-19 within the community. Furthermore, research work in [35] reveals that people with active or latent tuberculosis are more vulnerable to COVID-19. According to the report, the authors observed a more rapid and severe progression of symptoms in patients with both diseases. Clinical evidence indicates that TB is associated with COVID-19, resulting in a two to three-fold increase in mortality and a 25% relative reduction in the likelihood of recovery for individuals co-infected with both diseases [25].

Several research studies have shown that COVID-19 and tuberculosis rapidly transmit through close contact ([18], [40], [47]). Both these diseases primarily transmits rapidly in settings where there is close and prolonged contact between infected individuals and susceptible individuals. Some specific contexts where COVID-19 and tuberculosis transmission can occur rapidly include: poor ventilation, crowded places, and superspreading events. The implementation of the non-pharmaceutical interventions, such as isolation or quarantine help effectively mitigate the COVID-19 outbreak ([5],[15], [46], [47]). These measures are taken to prevent the potential spread of the disease by isolating and monitoring individuals during the incubation period or when they show symptoms. Quarantine typically involves staying in a designated location, such as a healthcare facility or one's

own home, and avoiding contact with others until the risk of spreading the disease has passed. It is an important public health strategy to control infectious diseases and protect the community. Hence, the quarantine measures plays a crucial role in mitigating the spread of co-infection between COVID-19 and tuberculosis.

Amidst the chaotic spread of COVID-19, there has been a concerning neglect of several other diseases, including tuberculosis, in terms of treatment and care. The significant surge in COVID-19 cases has led to a drastic decline in the identification and reporting of TB cases, consequently reversing the progress made towards the global TB targets. It is of utmost importance to prioritize the implementation of essential control measures, particularly in managing tuberculosis cases. This entails promptly identifying and managing COVID-19 in individuals with tuberculosis, giving them precedence in tuberculosis hospitals and medication centers. To prevent the escalating number of individuals co-infected with COVID-19 and tuberculosis, it is essential to implement quarantine measures. Several recent models have explored the dynamics of COVID-19 and tuberculosis (TB) co-infection. Studies have focused on vaccination and optimal control strategies without explicitly modeling quarantine ([1], [11]). Other works incorporated vaccination and isolation interventions, but did not systematically address quarantine for co-infected individuals ([17], [33]). Additional studies analyzed disease dynamics and sensitivity but lacked a quarantine component ([24], [26]). In contrast, the present study introduces quarantine compartments for individuals with COVID-19, TB, and co-infection, allowing a detailed assessment of quarantine as a non-pharmaceutical intervention. This study develops a mathematical model that systematically examines the impact of quarantine measures on the transmission dynamics of COVID-19 and tuberculosis co-infection, providing new insights into effective control strategies and the potential eradication of co-infections, thereby addressing a critical gap in the existing literature.

2. Model Formulation

We developed a mathematical model to study the dynamics of COVID-19 and tuberculosis co-infection, dividing the human population into 11 compartments based on the health status of individuals: susceptible individuals (S), exposed individuals with COVID-19 only (E_C), exposed individuals with tuberculosis only (E_T), individuals exposed with both COVID-19 and tuberculosis (E_{CT}), infected individuals with COVID-19 only (I_C), infected individuals with tuberculosis only (I_T), infected individuals with both COVID-19 and tuberculosis (I_{CT}), quarantined individuals with COVID-19 only (Q_C), quarantined individuals with tuberculosis only (Q_T), quarantined individuals with COVID-19 and tuberculosis only (Q_{CT}), and recovered individuals (R). The human population N at time t is $N(t) = S(t)+E_C(t)+E_T(t)+E_{CT}(t)+I_C(t)+I_T(t)+I_{CT}(t)+Q_C(t)+Q_T(t)+Q_{CT}(t)+R(t)$. The model has the following assumptions: individuals infected with COVID-19 only I_C are susceptible to tuberculosis infection and vice versa ([14], [17]); co-infected individuals I_{CT} can transmit either COVID-19 or tuberculosis but not the mixed infections at the same time ([14], [17]); co-infected individuals can recover either from COVID-19 or tuberculosis but not from the mixed infection at the same time ([14], [17], [27]); the trans-

missibility rates for single and co-infections are the same [14]; and recovered individuals R acquire lifelong immunity to both COVID-19 and tuberculosis. Every individual in all compartments may die naturally at a rate μ.

More specifically, individuals enter the susceptible compartment at a recruitment rate ω; upon exposure to individuals from compartments E_C and I_C, they transition to compartment E_C; while contact with individuals from compartment I_T may lead to movement to compartment E_T. Within compartment E_C, individuals may progress to compartment I_C at a rate r_c; some may transition to compartment E_{CT} upon exposure to individuals from compartment I_T; or some may move to compartment Q_C at a rate δ_e. Now, individuals in compartment I_C may die due to COVID-19 at a rate μ_1; and some may move to compartment Q_C at rate δ_c. Individuals in compartment Q_C may recover from COVID-19 at a rate γ_c; and some may die due to COVID-19 at a rate μ_4. Once in compartment E_T, individuals may move to compartment E_{CT} following contact with individuals from E_C and I_C; or some may transfer to compartment I_T at a rate r_t. Individuals in compartment I_T may move to compartment Q_T at a rate δ_t; and some may die due to tuberculosis at a rate μ_3. Meanwhile, individuals in compartment Q_T may recover at a rate γ_t; and some may die due to tuberculosis at a rate μ_5. Individuals in E_{CT} may move to compartment I_{CT} at rate r. On the other hand, individuals in Q_{CT} may move to compartment Q_C at a rate γ_{ct}; some may move to compartment Q_T at a rate γ_{tc}; and some may die due to co-infection at a rate μ_6.

Based on the aforementioned assumptions, Figure 1 presents the mathematical model depicting the transmission dynamics of COVID-19 and tuberculosis co-infection.

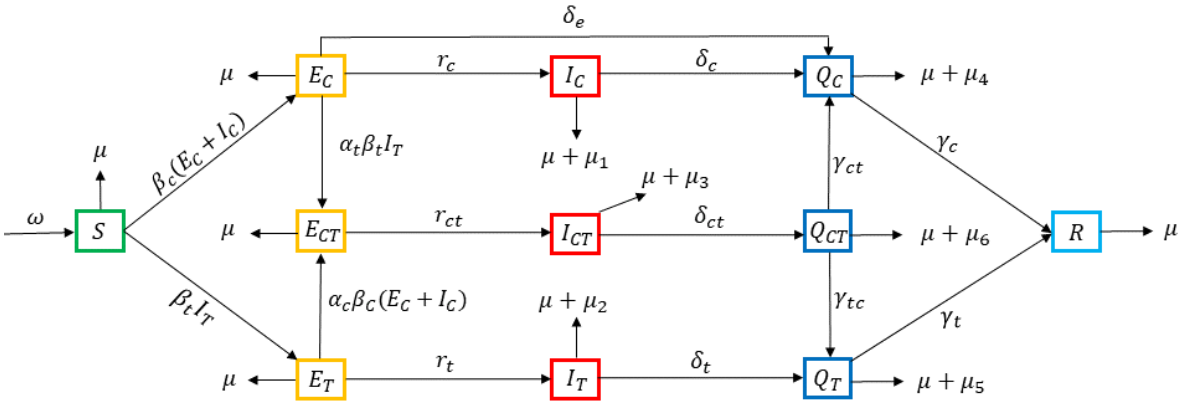

Figure 1: Transmission Dynamics of COVID-19 and TB Co-infection Model

The transmission dynamics of the COVID-19 and tuberculosis co-infection model, shown in Figure 1, are described by the following system of ordinary differential equations.

$$
\begin{cases}
\dfrac{dS}{dt} = \omega - \beta_c(E_C + I_C)S - \beta_t I_T S - \mu S \\
\dfrac{dE_C}{dt} = \beta_c(E_C + I_C)S - \alpha_t\beta_t I_T E_C - (r_c + \delta_e + \mu)E_C \\
\dfrac{dI_C}{dt} = r_c E_C - (\delta_c + \mu + \mu_1)I_C \\
\dfrac{dQ_C}{dt} = \delta_e E_C + \delta_c I_C + \gamma_{ct} Q_{CT} - (\gamma_c + \mu + \mu_4)Q_C \\
\dfrac{dE_{CT}}{dt} = \alpha_t\beta_t I_T E_C + \alpha_c\beta_c(E_C + I_C)E_T - (r_{ct} + \mu)E_{CT} \\
\dfrac{dI_{CT}}{dt} = r_{ct} E_{CT} - (\delta_{ct} + \mu + \mu_3)I_{CT} \\
\dfrac{dQ_{CT}}{dt} = \delta_{ct} I_{CT} - (\gamma_{tc} + \gamma_{ct} + \mu + \mu_6)Q_{CT} \\
\dfrac{dE_T}{dt} = \beta_t I_T S - \alpha_c\beta_c(E_C + I_C)E_T - (r_t + \mu)E_T \\
\dfrac{dI_T}{dt} = r_t E_T - (\delta_t + \mu + \mu_2)I_T, \\
\dfrac{dQ_T}{dt} = \delta_t I_T + \gamma_{tc} Q_{CT} - (\gamma_t + \mu + \mu_5)Q_T \\
\dfrac{dR}{dt} = \gamma_c Q_C + \gamma_t Q_T - \mu R.
\end{cases} \tag{1}
$$

Parameter	Description	Value	Source
ω	Recruitment rate	[2,4] day^{-1}	Assumed
β_c	Effective contact rate transmission of COVID-19	0.015	Assumed
β_t	Effective contact rate transmission of tuberculosis	0.012	Assumed
α_c	COVID-19 co-infection rate from TB exposure	1 day^{-1}	[14]
α_t	Tuberculosis co-infection rate from COVID-19 exposure	1 day^{-1}	[14]
r_c	Progression rate from asymptomatic to symptomatic COVID-19	0.33 day^{-1}	[23]
r_t	Progression rate from asymptomatic to symptomatic tuberculosis	0.7 day^{-1}	Assumed
r_{ct}	Progression rate from asymptomatic to symptomatic co-infection	0.02 day^{-1}	[23]
δ_e	Rate at which exposed individuals are isolated in COVID-19 quarantine	[0,1) day^{-1}	Assumed
δ_c	Rate at which infected individuals are isolated in COVID-19 quarantine	[0,1) day^{-1}	Assumed
δ_t	Rate at which infected individuals are isolated in TB quarantine	[0,1) day^{-1}	Assumed
δ_{ct}	Rate at which co-infected individuals are isolated in co-infected quarantine	0.79 day^{-1}	Assumed
γ_{ct}	Recovery rate of COVID-19 from co-infection	0.68 day^{-1}	Assumed
γ_{tc}	Recovery rate of TB from co-infection	0.35 day^{-1}	Assumed
γ_c	Recovery rate from COVID-19 infection	0.3 day^{-1}	[17]
γ_t	Recovery rate from tuberculosis infection	0.2 day^{-1}	[17]
μ	Natural death rate	0.0477 day^{-1}	[23]
μ_1	Death rate of COVID-19 infected individuals	0.23 day^{-1}	[23]
μ_2	Death rate of tuberculosis infected individuals	0.01 day^{-1}	[23]
μ_3	Death rate of co-infected individuals	0.03 day^{-1}	[17]
μ_4	Death rate of COVID-19 infected individuals in quarantine	0.23 day^{-1}	[23]
μ_5	Death rate of tuberculosis infected individuals in quarantine	0.004 day^{-1}	[17]
μ_6	Death rate of co-infected individuals in quarantine	0.03 day^{-1}	[17]

Table 1: Description of the Model Parameters

System (1) is defined with the following initial conditions $S(0) \geq 0$, $E_C(0) \geq 0$, $I_C(0) \geq 0$, $Q_C(0) \geq 0$, $E_{CT}(0) \geq 0$, $I_{CT}(0) \geq 0$, $Q_{CT}(0) \geq 0$, $E_T(0) \geq 0$, $I_T(0) \geq 0$, $Q_T(0) \geq 0$, and $R(0) \geq 0$. All parameters in system (1) are described in Table 1.

3. Model Analysis

This section examines the analysis of three models: the COVID-19 sub-model, the tuberculosis sub-model, and the co-infection model.

3.1. COVID-19 Sub-model

Without considering tuberculosis-infected individuals from the co-infection model, the COVID-19 sub-model is given by

$$\begin{cases} \dfrac{dS}{dt} = \omega - \beta_c(E_C + I_C)S - \mu S \\ \dfrac{dE_C}{dt} = \beta_c(E_C + I_C)S - (r_c + \delta_e + \mu)E_C \\ \dfrac{dI_C}{dt} = r_c E_C - (\delta_c + \mu + \mu_1)I_C \\ \dfrac{dQ_C}{dt} = \delta_e E_C + \delta_c I_C - (\gamma_c + \mu + \mu_4)Q_C \\ \dfrac{dR}{dt} = \gamma_c Q_C - \mu R, \end{cases} \tag{2}$$

where $N_C = S + E_C + I_C + Q_C + R$. By adding all the equations in the system (2), we obtained $\omega - \mu N_C - \mu_1 I_C - \mu_4 Q_C \leq \omega - \mu N_C$. The given initial conditions of the COVID-19 sub-model system (2) guarantee that $N(0) \geq 0$. Thus, the total human population is positive and bounded for finite time $t > 0$. By differential inequality [4], $N_C(t) \leq N_C(0)e^{-\mu t} + \frac{\omega}{\mu}(1 - e^{-\mu t})$. As $t \to +\infty$, we get $0 \leq N_C(t) \leq \frac{\omega}{\mu}$. The feasible region of the COVID-19 sub-model (2) is given by $\Omega_C = \left\{(S, E_C, I_C, Q_C, R) \in \mathbb{R}^5_+ : N_C(t) \leq \frac{\omega}{\mu}\right\}$. The set Ω_C is positive invariant and attracting [16], and all the solutions of the COVID-19 sub-model (2) starting in Ω_C remain in Ω_C for all $t \geq 0$. Thus, the model (2) is mathematically and epidemiologically well-posed, and is sufficient to study its dynamics in Ω_C.

Note that the first four (4) equations in system (2) are independent of the last equation, which means that R has no effect on the system. Without loss of generality, the last equation can be omitted from the system. Now, setting all differential equations in system (2) to zero and solving for all compartments, we obtain two equilibrium points, the disease-free equilibrium (DFE) and the endemic equilibrium (EE). The disease-free equilibrium point is obtained when $E_C = 0$ and $I_C = 0$ and will be denoted by

$$E_{0_C} = (S, E_C, I_C, Q_C) = \left(\frac{\omega}{\mu}, 0, 0, 0\right). \tag{3}$$

When $E_C \neq 0$ and $I_C \neq 0$, the endemic equilibrium point exists and is given by $E_{1_C} = (S, E_C, I_C, Q_C)$ where

$$\begin{aligned}
S &= \frac{(r_c+\delta_e+\mu)(\delta_c+\mu+\mu_1)}{\beta_c(\delta_c+\mu+\mu_1+r_c)} \\
E_C &= \frac{\omega\beta_c(\delta_c+\mu+\mu_1+r_c)-\mu(r_c+\delta_e+\mu)(\delta_c+\mu+\mu_1)}{\beta_c(r_c+\delta_e+\mu)(\delta_c+\mu+\mu_1+r_c)} \\
I_C &= \frac{r_c\omega\beta_c(\delta_c+\mu+\mu_1+r_c)-r_c\mu(r_c+\delta_e+\mu)(\delta_c+\mu+\mu_1)}{\beta_c(r_c+\delta_e+\mu)(\delta_c+\mu+\mu_1+r_c)(\delta_c+\mu+\mu_1)} \\
Q_C &= \frac{\delta_e\omega\beta_c(\delta_c+\mu+\mu_1+r_c)-\delta_e\mu(r_c+\delta_e+\mu)(\delta_c+\mu+\mu_1)}{\beta_c(r_c+\delta_e+\mu)(\delta_c+\mu+\mu_1+r_c)(\gamma_c+\mu+\mu_4)} \\
&\quad + \frac{\delta_c r_c\omega\beta_c(\delta_c+\mu+\mu_1+r_c)-\delta_c r_c\mu(r_c+\delta_e+\mu)(\delta_c+\mu+\mu_1)}{\beta_c(r_c+\delta_e+\mu)(\delta_c+\mu+\mu_1+r_c)(\delta_c+\mu+\mu_1)(\gamma_c+\mu+\mu_4)}.
\end{aligned} \tag{4}$$

The basic reproduction number (R_0) is defined as the average number of secondary infections produced by a single COVID-19-infected individual in a completely susceptible population [44]. The Next Generation Matrix (NGM) is used to compute the basic reproduction number. The system (2) can be written as $\dot{x} = f(x) = \mathcal{F}(x) - \mathcal{V}(x)$ where $\mathcal{F}$ is the transmission matrix and the $\mathcal{V}$ is the transition matrix are given as follows

$$\mathcal{F} = \begin{pmatrix} \beta_c(E_C+I_C)S \\ 0 \\ 0 \end{pmatrix} \quad \text{and} \quad \mathcal{V} = \begin{pmatrix} (r_c+\delta_e+\mu)E_C \\ -r_cE_C+(\delta_c+\mu+\mu_1)I_C \\ -\delta_eE_C-\delta_cI_C+(\gamma_c+\mu+\mu_4)Q_C \end{pmatrix}.$$

Evaluating the Jacobian matrix of $\mathcal{F}$ and $\mathcal{V}$ at the disease-free equilibrium E_{0_C} gives

$$F = \begin{pmatrix} \frac{\beta_c\omega}{\mu} & \frac{\beta_c\omega}{\mu} & 0 \\ 0 & 0 & 0 \\ 0 & 0 & 0 \end{pmatrix} \quad \text{and} \quad V = \begin{pmatrix} r_c+\delta_e+\mu & 0 & 0 \\ -r_c & \delta_c+\mu+\mu_1 & 0 \\ -\delta_e & -\delta_c & \gamma_c+\mu+\mu_4 \end{pmatrix},$$

respectively. Let

$$A_1 = r_c+\delta_e+\mu,\ A_2 = \delta_c+\mu+\mu_1,\ \text{and } A_3 = \gamma_c+\mu+\mu_4. \tag{5}$$

Then

$$V^{-1} = \begin{pmatrix} \frac{1}{A_1} & 0 & 0 \\ \frac{r_c}{A_1A_2} & \frac{1}{A_2} & 0 \\ \frac{\delta_cr_c+\delta_eA_2}{A_1A_2A_3} & \frac{\delta_c}{A_2A_3} & \frac{1}{A_3} \end{pmatrix}.$$

Consequently,

$$FV^{-1} = \begin{pmatrix} \frac{\beta_c\omega}{\mu A_1}+\frac{\beta_c\omega r_c}{\mu A_1A_2} & \frac{\beta_c\omega}{\omega A_2} & 0 \\ 0 & 0 & 0 \\ 0 & 0 & 0 \end{pmatrix}.$$

Accordingly, the largest eigenvalue of FV^{-1} is $\frac{\beta_c\omega}{\mu A_1}+\frac{\beta_c\omega r_c}{\mu A_1 A_2}$. Hence, the basic reproduction number of the COVID-19 sub-model (2) is given by

$$R_{0_C}=\frac{\beta_c\omega}{\mu(r_c+\delta_e+\mu)}+\frac{\beta_c\omega r_c}{\mu(r_c+\delta_e+\mu)(\delta_c+\mu+\mu_1)}.$$

This quantity is a crucial epidemiological metric that indicates the potential spread of an infectious disease within a population. It determines whether the disease will continue to spread ($R_{0_C}>1$) or eventually decline ($R_{0_C}<1$) in the community. Hence, this will guide public health strategies and intervention measures.

3.2. Stability Analysis of the Equilibrium Points for the COVID-19 Sub-model

This subsection examines the stability of the equilibrium points for the COVID-19 sub-model (2).

Theorem 1. *If $R_{0_C}<1$, then the COVID-19 sub-model (2) is locally asymptotically stable at the disease-free equilibrium E_{O_C} and unstable otherwise.*

Proof. The Jacobian matrix of system (2) evaluated at E_{O_C} is given by

$$J_{E_{O_C}}=\begin{pmatrix}-\mu & \frac{-\beta_c\omega}{\mu} & \frac{-\beta_c\omega}{\mu} & 0\\ 0 & \frac{\beta_c\omega}{\mu}-A_1 & \frac{\beta_c\omega}{\mu} & 0\\ 0 & r_c & -A_2 & 0\\ 0 & \delta_e & \delta_c & -A_3\end{pmatrix},$$

where A_i, A_2, and A_3 are given in (5). Then the characteristic polynomial of the Jacobian matrix $J_{E_{O_C}}$ is

$$J_{E_{O_C}}(\lambda)=(-\mu-\lambda)(-A_3-\lambda)\left[\lambda^2+\Big(A_1+A_2-\frac{\beta_c\omega}{\mu}\Big)\lambda+A_1A_2-\frac{\beta_c\omega(A_2-r_c)}{\mu}\right].$$

Hence, the characteristic roots are $\lambda_1=-\mu$ and $\lambda_2=-A_3$ and the other roots are determined by the remaining factor

$$\lambda^2+\Big(A_1+A_2-\frac{\beta_c\omega}{\mu}\Big)\lambda+A_1A_2-\frac{\beta_c\omega(A_2-r_c)}{\mu}.$$

Observe that when $R_{0_C}<1$, $A_1+A_2-\frac{\beta_c\omega}{\mu}>0$. Moreover,

$$A_1A_2-\frac{\beta_c\omega(A_2-r_c)}{\mu}=A_1A_2(1-R_{0_C})>0$$

when $R_{0_C}<1$. By Routh-Hurwitz criterion, all eigenvalues of the second order polynomial are negative, which means that COVID-19 sub-model system (2) is locally asymptotically stable at E_{0_C} when $R_{0_C}<1$ and unstable otherwise.

Theorem 2. *If $R_{0_C} < 1$, then the COVID-19 sub-model (2) is globally asymptotically stable at disease-free equilibrium E_{0_C}.*

Proof. Consider the Lyapunov function below

$$L = (\delta_c + \mu + \mu_1)E_C + \Big(\frac{\beta_c\omega}{\mu}\Big)I_C.$$

The time derivative of L computed along the solution of (2) is negative definite. That is,

$$\begin{aligned}
\dot{L} &= (\delta_c + \mu + \mu_1)E_C' + \Big(\frac{\beta_c\omega}{\mu}\Big)I_C' \\
&= (\delta_c + \mu + \mu_1)\Big[\beta_c(E_C + I_C)S - (r_c + \delta_e + \mu)E_C\Big] + \Big(\frac{\beta_c\omega}{\mu}\Big)\Big[r_cE_C - (\delta_c + \mu + \mu_1)I_C\Big] \\
&\leq (\delta_c + \mu + \mu_1)\Big[\beta_c(E_C + I_C)\frac{\omega}{\mu} - (r_c + \delta_e + \mu)E_C\Big] + \Big(\frac{\beta_c\omega}{\mu}\Big)\Big[r_cE_C - (\delta_c + \mu + \mu_1)I_C\Big] \\
&= \frac{\beta_c\omega(\delta_c + \mu + \mu_1)E_C}{\mu} - (\delta_c + \mu + \mu_1)(r_c + \delta_e + \mu)E_C + \frac{\beta_c\omega r_cE_C}{\mu} \\
&= \frac{\beta_c\omega(\delta_c + \mu + \mu_1 + r_c)E_C}{\mu} - (\delta_c + \mu + \mu_1)(r_c + \delta_e + \mu)E_C \\
&= \big[(\delta_c + \mu + \mu_1)(r_c + \delta_e + \mu)E_C\big](R_{0_C} - 1) \\
&\leq 0 \ \text{ if } \ R_{0_C} < 1.
\end{aligned}$$

Because all model parameters are non-negative, it follows that $\dot{L}$ is negative semi-definite, that is, $\dot{L} \leq 0$ if $R_{0_C} < 1$. If the solution $x^* = E_{0_C}$, then $\dot{L} = 0$. Conversely, if $\dot{L} = 0$, then $S = \frac{\omega}{\mu}$, $E_C = 0$ $I_C = 0$ and $Q_C = 0$. Hence, $\dot{L} = 0$ if and only if $x^* = E_{0_C}$. So, $\dot{L}$ is a Lyapunov function on Ω_c and the largest compact invariant set in $\{(S, E_C, I_C, Q_C) \in \Omega_c : \dot{L} = 0\}$ is $\{(\frac{\omega}{\mu}, 0, 0, 0)\}$. Thus, by LaSalle's invariance principle, every solution of system (2) with the initial conditions in Ω_c approaches $E_{0_C} = (\frac{\omega}{\mu}, 0, 0, 0)$ at $t \to \infty$ whenever $R_{0_C} < 1$. Therefore, the COVID-19 sub-model (2) is globally asymptotically stable at the disease-free equilibrium point $E_{0_C} = (\frac{\omega}{\mu}, 0, 0, 0)$ if $R_{0_C} < 1$.

The next result shows the existence of a unique positive endemic equilibrium for the COVID-19 sub-model (2). Note that the positive endemic equilibrium for the COVID-19 sub-model (2) can be expressed in terms of R_{0_C}, that is,

$$S^* = \frac{\omega}{\mu R_{0_C}}, \quad E_C^* = \frac{\omega(R_{0_C} - 1)}{(r_c + \delta_e + \mu)R_{0_C}}, \quad I_C^* = \frac{r_c\omega(R_{0_C} - 1)}{(r_c + \delta_e + \mu)R_{0_C}(\delta_c + \mu + \mu_1)}, \quad \text{and}$$

$$Q_C^* = \frac{(R_{0_C} - 1)(\delta_e\omega(\delta_c + \mu + \mu_1) + \delta_c r_c\omega)}{(r_c + \delta_e + \mu)R_{0_C}(\delta_c + \mu + \mu_1)(\gamma_c + \mu + \mu_1)}.$$

Hence, we have the following result.

Theorem 3. *If $R_{0_C} > 1$, then the COVID-19 sub-model (2) has a unique positive endemic equilibrium.*

Theorem 4. *If $R_{0_C} > 1$, then the COVID-19 sub-model (2) is locally asymptotically stable at the endemic equilibrium E_{1_C} and unstable otherwise.*

Proof. The Jacobian matrix of system (2) evaluated at the endemic equilibrium point E_{1_C} is given by

$$J_{E_{1_C}} = \begin{bmatrix} -\beta_c(E_C^* + I_C^*) - \mu & -\beta_c S^* & -\beta_c S^* & 0 \\ \beta_c(E_C^* + I_C^*) & \beta_c S^* - A_1 & \beta_c S^* & 0 \\ 0 & r_c & -A_2 & 0 \\ 0 & \delta_e & \delta_c & -A_3 \end{bmatrix},$$

where A_1, A_2 and A_3 are given in (5). Then the characteristic polynomial of $J_{E_{1_C}}$ is

$$\begin{aligned} J_{E_{1_C}}(\lambda) =& (-A_3 - \lambda)\Big(\lambda^3 - (-A_2 + \beta_c S^* - A_1 - \beta_c E^* - \beta_c I^* - \mu)\lambda^2 - (-\beta_c A_1 E^* - \beta_c A_1 I^* - \beta_c A_2 E^* - \beta_c A_2 I^* \\ &+ \beta_c A_2 S^* + \beta_c \mu S^* + \beta_c r_c S^* - A_1 A_2 - \mu A_1 - \mu A_2)\lambda + \beta_c A_1 A_2 I^* - \beta_c \mu A_2 S^* - \beta_c \mu r_c S^* + \mu A_1 A_2\Big) \end{aligned}$$

Certainly, the eigenvalue $\lambda = -A_3 < 0$. The other eigenvalues are determined by the cubic polynomial factor. Set the coefficients and constant term of the cubic polynomial as follows: a_1 as the coefficient of λ^2, a_2 as the coefficient of λ and a_3 as the constant term. By Routh Hurwitz criterion, the eigenvalues that are determined by cubic polynomial have negative real parts if the following conditions are satisfied: a_1, a_2, and a_3 are all positive and $a_1 a_2 > a_3$. By Theorem (3), a_1, a_2, and a_3 can be expressed as

$$\begin{aligned} a_1 &= A_2 + \frac{\beta_c \omega r_c A_1}{\beta_c \omega A_2 + \beta_c \omega r_c} + \frac{\beta_c \omega (R_{0_C} - 1)}{A_1 R_{0_C}} + \frac{\beta_c r_c \omega (R_{0_C} - 1)}{A_1 R_{0_C}} + \mu \\ a_2 &= \frac{\beta_c \omega (R_{0_C} - 1)}{R_{0_C}} + \frac{\beta_c r_c \omega (R_{0_C} - 1)}{A_2 R_{0_C}} + \frac{\beta_c \omega A_2 (R_{0_C} - 1)}{A_1 R_{0_C}} + \frac{\beta_c r_c \omega (R_{0_C} - 1)}{A_1 R_{0_C}} + \frac{\beta_c \omega r_c \mu A_1}{\beta_c \omega A_2 + \beta_c \omega r_c} + \mu A_2 \\ a_3 &= \frac{\beta_c \omega A_2 (R_{0_C} - 1)}{R_{0_C}} + \frac{\beta_c r_c \omega (R_{0_C} - 1)}{R_{0_C}} \end{aligned}$$

Moreover,

$$a_1 a_2 = \frac{\beta_c \omega A_2 (R_{0_C} - 1)}{R_{0_C}} + \frac{\beta_c r_c \omega (R_{0_C} - 1)}{R_{0_C}} + \Delta = a_3 + \Delta,$$

where

$$\begin{aligned} \Delta =& A_2\Big(\frac{\beta_c \omega A_2 (R_{0_C} - 1)}{A_1 R_{0_C}} + \frac{\beta_c r_c \omega (R_{0_C} - 1)}{A_1 R_{0_C}} + \frac{\beta_c \omega r_c \mu A_1}{\beta_c \omega A_2 + \beta_c \omega r_c} + \mu A_2\Big) \\ &+ a_2\Big(\frac{\beta_c \omega r_c A_1}{\beta_c \omega A_2 + \beta_c \omega r_c} + \frac{\beta_c \omega (R_{0_C} - 1)}{A_1 R_{0_C}} + \frac{\beta_c r_c \omega (R_{0_C} - 1)}{A_1 R_{0_C}} + \mu\Big) \end{aligned}$$

Note that a_1, a_2 and a_3 are all positive and $a_1 a_2 > a_3$ if $R_{0_C} > 1$. Hence, the COVID-19 sub-model (2) is locally asymptotically stable at the endemic equilibrium point E_{1_C} when $R_{0_C} > 1$ and unstable otherwise.

3.3. Sensitivity Analysis of COVID-19 Sub-model

In this subsection, sensitivity analysis of the parameters in the COVID-19 sub-model is performed. The sensitivity of a parameter p is defined as the behavior of the model to a small change in its parameter value [22], and is given by

$$S_p = \frac{\partial R_{0_C}}{\partial p} \times \frac{p}{R_{0_C}}, \quad \text{where} \quad R_{0_C} = \frac{\beta_c \omega}{\mu(r_c + \epsilon_C + \mu)} + \frac{\beta_c \omega r_c}{\mu(r_c + \epsilon_C + \mu)(\rho_C + \mu + \sigma_C)} \tag{6}$$

The sensitivity indices for each parameter in the COVID-19 sub-model (2) with respect to R_{0_C} is computed using the equation (6), and the corresponding sensitivity indices are shown in Figure 2.

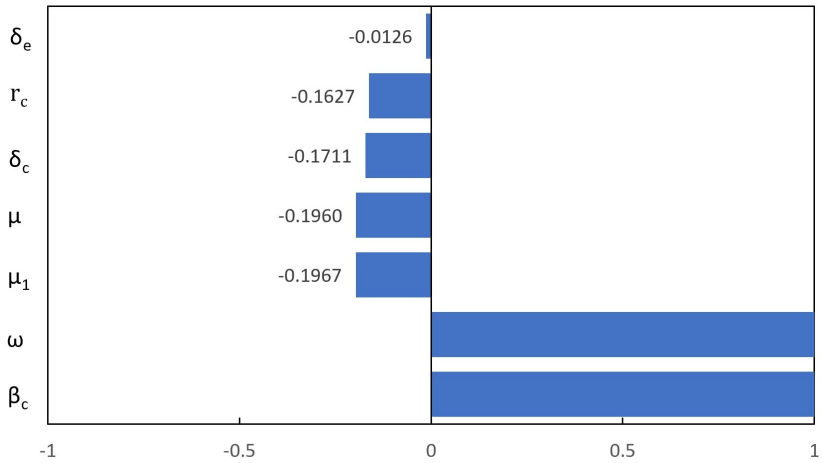

Figure 2: Sensitivity indices of the COVID-19 sub-model parameters

The sensitivity analysis of the COVID-19 sub-model numerical results highlighted that the COVID-19 transmission rate β_c, and the recruitment rate ω have a high positive impact on the spread of the virus. The analysis suggests that the magnitude of the impacts of β_c and ω on the spread of COVID-19 are the same because the number of secondary infections increase with respect to increasing these parameters [22]. In contrast, the parameters μ_1, μ, δ_c, r_c, and δ_e have negative impact, which means that increasing the value of such parameters will decrease the number of people infected with COVID-19.

3.4. Tuberculosis Sub-model

Without considering the infected individuals with COVID-19 from the COVID-19 and tuberculosis co-infection model (1), the tuberculosis sub-model is given by

$$\begin{cases} \dfrac{dS}{dt} = \omega - \beta_t I_T S - \mu S \\ \dfrac{dE_T}{dt} = \beta_t I_T S - (r_t + \mu) E_T \\ \dfrac{dI_T}{dt} = r_t E_T - (\delta_t + \mu + \mu_2) I_T \\ \dfrac{dQ_T}{dt} = \delta_t I_T - (\gamma_t + \mu + \mu_5) Q_T \\ \dfrac{dR}{dt} = \gamma_t Q_T - \mu R \end{cases} \tag{7}$$

where $N_T = S + E_T + I_T + Q_T + R$. By adding all the equations in system (7), we obtained $\omega - \mu N_T - \mu_2 I_T - \mu_5 Q_T \leq \omega - \mu N_T$. The given initial conditions of the tuberculosis sub-model system (7) ensure that $N(0) \geq 0$. Hence, the total human population is positive and bounded for all finite time $t > 0$. From the theory of differential inequality [4], $N_T(t) \leq N_T(0)e^{-\mu t} + \frac{\omega}{\mu}(1 - e^{-\mu t})$. As $t \to +\infty$, we get $0 \leq N_T(t) \leq \frac{\omega}{\mu}$. The feasible region of the TB sub-model (7) is given by $\Omega_T = \left\{(S, E_T, I_T, Q_T, R) \in \mathbb{R}^5_+ : N_T(t) \leq \frac{\omega}{\mu}\right\}$. The set Ω_C is positive invariant and attracting [16], and all solutions of the tuberculosis sub-model (7) starting in Ω_T remain in Ω_T for all $t \geq 0$. Hence, the model (7) is mathematically and epidemiologically well-posed, and it is sufficient to study its dynamics in Ω_T.

Without loss of generality, the last equation can be omitted since it is independent of the system (7). Setting all the differential equations in system (7) to zero and solve for all compartments, we obtain two equilibrium points, the disease-free equilibrium (DFE) and the endemic equilibrium (EE). The disease-free equilibrium point is obtained when $E_T = 0$ and $I_T = 0$ and given by

$$E_{0_T} = (S, E_T, I_T, Q_T) = \left(\frac{\omega}{\mu}, 0, 0, 0\right).$$

When $E_T \neq 0$ and $I_T \neq 0$, the endemic equilibrium point exists and is given by $E_{1_T} = (S, E_T, I_T, Q_T)$ where

$$S = \frac{(\mu + r_t)(\delta_t + \mu + \mu_2)}{\beta_t r_t}, \quad E_T = \frac{\omega\beta_t r_t - \mu(\mu + r_t)(\delta_t + \mu + \mu_2)}{(\beta_t r_t)(r_t + \mu)},$$

$$I_T = \frac{\omega\beta_t r_t - \mu(\mu + r_t)(\delta_t + \mu + \mu_2)}{\beta_t(r_t + \mu)(\delta_t + \mu + \mu_2)}, \quad Q_T = \frac{\delta_t(\omega\beta_t r_t - \mu(\mu + r_t)(\delta_t + \mu + \mu_2))}{\beta_t(r_t + \mu)(\delta_t + \mu + \mu_2)(\gamma_t + \mu + \mu_5)}.$$

This completes the solution for the existence of the equilibrium points for the tuberculosis sub-model (7).

The basic reproduction number of the tuberculosis sub-model R_{0_T} is obtained using the next generation matrix [12]. The $\mathcal{F}$ is the transmission matrix and the $\mathcal{V}$ is the transition matrix of the system (7) are given as follows

$$\mathcal{F} = \begin{pmatrix} \beta_t I_T S \\ 0 \\ 0 \end{pmatrix} \text{ and } \mathcal{V} = \begin{pmatrix} (r_t + \mu)E_T \\ -r_t E_T + (\delta_t + \mu + \mu_2)I_T \\ -\delta_t I_T + (\gamma_t + \mu + \mu_5)Q_T \end{pmatrix}.$$

Then the Jacobian matrix of $\mathcal{F}$ and $\mathcal{V}$ evaluated in the disease-free equilibrium E_{0_T}

$$F = \begin{pmatrix} 0 & \frac{\beta_t \omega}{\mu} & 0 \\ 0 & 0 & 0 \\ 0 & 0 & 0 \end{pmatrix} \quad \text{and} \quad V = \begin{pmatrix} r_t + \mu & 0 & 0 \\ -r_t & \delta_t + \mu + \mu_2 & 0 \\ 0 & -\delta_t & \gamma_t + \mu + \mu_5 \end{pmatrix}.$$

Setting

$$B_1 = r_t + \mu,\ B_2 = \delta_t + \mu + \mu_2,\ B_3 = \gamma_t + \mu + \mu_5 \tag{8}$$

Hence,

$$V^{-1} = \begin{pmatrix} \frac{1}{B_1} & 0 & 0 \\ \frac{r_t}{B_1 B_2} & \frac{1}{B_2} & 0 \\ \frac{\delta_t r_t}{B_1 B_2 B_3} & \frac{\delta_t}{B_2 B_3} & \frac{1}{B_3} \end{pmatrix}.$$

Consequently,

$$FV^{-1} = \begin{pmatrix} \frac{\beta_t \omega r_t}{\mu B_1 B_2} & \frac{\beta_t \omega}{\mu B_2} & 0 \\ 0 & 0 & 0 \\ 0 & 0 & 0 \end{pmatrix}.$$

Accordingly, the largest eigenvalue of $FV^{-1}(\lambda)$ is $\frac{\beta_t \omega r_t}{\mu B_1 B_2}$. Thus, the basic reproduction number of the tuberculosis sub-model (7) is

$$R_{0_T} = \frac{\beta_t \omega r_t}{\mu(r_t + \mu)(\delta_t + \mu + \mu_2)}.$$

It is important to note that the endemic equilibrium can be expressed in terms of $R_{E_{O_T}}$, that is,

$$S^* = \frac{\omega}{\mu R_{0_T}},\ E_T^* = \frac{\omega(R_{0_T} - 1)}{(r_t + \mu)R_{0_T}},\ I_T^* = \frac{r_t \omega(R_{0_T} - 1)}{(r_t + \mu)R_{0_T}(\delta_t + \mu + \mu_2)},\ Q_T^* = \frac{\delta_t r_t \omega(R_{0_T} - 1)}{(r_t + \mu)R_{0_T}(\delta_t + \mu + \mu_2)(\gamma_t + \mu + \mu_5)}.$$

Hence, the unique positive endemic equilibrium for the tuberculosis sub-model (7) only exists when $R_{E_{O_T}} > 1$. In particular, we have the following result.

Theorem 5. *If $R_{0_T} > 1$, then the tuberculosis sub-model (7) has a unique positive endemic equilibrium.*

3.5. Stability Analysis of the Equilibrium Points for the Tuberculosis Sub-model

Theorem 6. *If $R_{0_T} < 1$, then the tuberculosis sub-model (7) is locally asymptotically stable at the disease-free equilibrium E_{O_T} and unstable otherwise.*

Proof. The Jacobian matrix of system (7) evaluated at disease-free equilibrium E_{0_T} is given by $J_{E_{0_T}} = \big(\frac{\omega}{\mu}, 0, 0, 0\big)$, that is

$$J_{E_{0_T}} = \begin{pmatrix} -\mu & 0 & \frac{-\beta_t\omega}{\mu} & 0 \\ 0 & -B_1 & \frac{\beta_t\omega}{\mu} & 0 \\ 0 & r_t & -B_2 & 0 \\ 0 & 0 & \delta_t & -B_3 \end{pmatrix},$$

where B_1, B_2 and B_3 are given in (8). The characteristic polynomial of the Jacobian matrix $J_{E_{0_T}}$ is

$$J_{E_{0_T}}(\lambda) = (-\mu - \lambda)(-B_3 - \lambda)\Big(\lambda^2 + (B_1 + B_2)\lambda + B_1B_2 - \frac{\beta_t\omega r_t}{\mu}\Big).$$

Certainly, the eigenvalues $\lambda = -\mu < 0$ and $\lambda = -B_3 < 0$. The other eigenvalues are determined by the second order polynomial factor which can be expressed as $\lambda^2 + (B_1 + B_2)\lambda + B_1B_2\Big(1 - R_{0_T}\Big)$. If $R_{0_T} < 1$, then the coefficient $B_1 + B_2$ and the constant term $B_1B_2\Big(1 - R_{0_T}\Big)$ are all positive. Hence, by Routh-Hurwitz criterion, the tuberculosis-only submodel (7) is locally asymptotically stable at the disease-free equilibrium point E_{0_T} when $R_{0_T} < 1$ and unstable otherwise.

Theorem 7. *If $R_{0_T} < 1$, then the tuberculosis sub-model (7) is globally asymptotically stable at the disease-free equilibrium E_{0_T}.*

Proof. Consider the Lyapunov function below

$$L = (\delta_t + \mu + \mu_2)E_T + \Big(\frac{\beta_t\omega}{\mu}\Big)I_T.$$

The time derivative of L computed along the solution of (7) is negative semi-definite, that is,

$$\begin{aligned}
\dot{L} &= (\delta_t + \mu + \mu_2){E'}_T(t) + \Big(\frac{\beta_t\omega}{\mu}\Big){I'}_T(t) \\
&= (\delta_t + \mu + \mu_2)\big[\beta_t I_T S - (r_t + \mu)E_T\big] + \Big(\frac{\beta_t\omega}{\mu}\Big)\Big[r_tE_T - (\delta_t + \mu + \mu_2)I_T\Big] \\
&\leq (\delta_t + \mu + \mu_2)\big[\beta_t I_T\Big(\frac{\omega}{\mu}\Big) - (r_t + \mu)E_T\big] + \Big(\frac{\beta_t\omega}{\mu}\Big)\Big[r_tE_T - (\delta_t + \mu + \mu_2)I_T\Big] \\
&= -(\delta_t + \mu + \mu_2)(r_t + \mu)E_T + \frac{\beta_t\omega r_tE_T}{\mu} \\
&= \big[(\delta_t + \mu + \mu_2)(r_t + \mu)E_T\big](R_{0_T} - 1) \\
&\leq 0 \ \text{ if } \ R_{0_T} < 1.
\end{aligned}$$

If the solution of the system is $x^* = E_{0_T}$, then $\dot{L} = 0$. Conversely, if $\dot{L} = 0$, then $S_T = \frac{\omega}{\mu}$, $I_T = 0$, $E_T = 0$ and $Q_T = 0$. Hence, $\dot{L} = 0$ if and only if $x^* = E_{0_T}$. So, L is a Lyapunov function on Ω_T and the largest compact invariant set in $\{(S, E_T, I_T, Q_T) \in \Omega_T : \dot{L} = 0\}$ is $\{(\frac{\omega}{\mu}, 0, 0, 0)\}$. Thus, by LaSalle's invariance principle, every solution of system (7) with the initial conditions in Ω_T approaches $E_{0_T} = (\frac{\omega}{\mu}, 0, 0, 0)$ at $t \to \infty$ whenever $R_{0_T} < 1$. Therefore, the tuberculosis sub-model (7) is globally asymptotically stable at the disease-free equilibrium point $E_{0_T} = (\frac{\omega}{\mu}, 0, 0, 0)$ when $R_{0_T} < 1$.

Theorem 8. *If $R_{0_T} > 1$, then the tuberculosis sub-model (7) is locally asymptotically stable at the endemic equilibrium point E_{1_T} and unstable otherwise.*

Proof. The Jacobian matrix of system (7) evaluated at the endemic equilibrium point E_{1_T} is given by

$$J_{E_{1_T}} = \begin{pmatrix} \frac{-(\omega\beta_t r_t - \mu B_1 B_2)}{B_1 B_2} - \mu & 0 & \frac{-B_1 B_2}{r_t} & 0 \\ \frac{\omega\beta_t r_t - \mu B_1 B_2}{B_1 B_2} & -B_1 & \frac{B_1 B_2}{r_t} & 0 \\ 0 & r_t & -B_2 & 0 \\ 0 & 0 & \delta_t & -B_3 \end{pmatrix},$$

where B_1, B_2 and B_3 are given in (8). Hence, the characteristic polynomial of $J_{E_{1_T}}$ is

$$J_{E_{1_T}}(\lambda) = (-B_3 - \lambda)\left(-\lambda^3 + \frac{(-B_1^2 B_2 - B_1 B_2^2 - \beta_t\omega r_t)\lambda^2}{B_1 B_2} + \frac{(-B_1\beta_t\omega r_t - B_2\beta_t\omega r_t)\lambda}{B_1 B_2} + \frac{(B_1^2 B_2^2\mu - B_1 B_2\beta_t\omega r_t)}{B_1 B_2}\right)$$

Certainly, the eigenvalue $\lambda = -B_3 < 0$. The other eigenvalues are determined by the cubic polynomial factor. Set the coefficients and constant term of the cubic polynomial as follows: b_1 as the coefficient of λ^2, b_2 as the coefficient of λ and b_3 as the constant term. By Routh Hurwitz criterion, the eigenvalues of the cubic polynomial have negative real parts when the following conditions are satisfied: b_1, b_2, and b_3 are all positive and $b_1 b_2 > b_3$. Now, b_1, b_2, and b_3 can be express as

$$b_1 = -\frac{(-B_1^2 B_2 - B_1 B_2^2 - \beta_t\omega r_t)}{B_1 B_2} = \frac{B_1^2 B_2 + B_1 B_2^2 + \beta_t\omega r_t}{B_1 B_2} > 0$$
$$b_2 = -\frac{(-B_1\beta_t\omega r_t - B_2\beta_t\omega r_t)}{B_1 B_2} = \frac{B_1\beta_t\omega r_t + B_2\beta_t\omega r_t}{B_1 B_2} > 0$$
$$b_3 = \beta_t\omega r_t - B_1 B_2\mu = B_1 B_2\mu\left(\frac{\beta_t\omega r_t}{B_1 B_2\mu} - 1\right) = B_1 B_2\mu(R_{0_T} - 1)$$

Hence, the tuberculosis sub-model (7) is locally asymptotically stable at the endemic equilibrium point E_{1_T} when $R_{0_T} > 1$ and unstable otherwise.

3.6. Sensitivity Analysis of Tuberculosis Sub-model

In this subsection, we conducted a sensitivity analysis of the parameters in the tuberculosis sub-model. For a parameter p, the sensitivity of p is defined as the behavior of the model to a small change in its value [22], and is given by:

$$S_p = \frac{\partial R_{0_T}}{\partial p} \times \frac{p}{R_{0_T}} \quad \text{where} \quad R_{0_T} = \frac{\beta_t\omega r_t}{\mu(r_t + \mu)(\delta_t + \mu + \mu_2)} \tag{9}$$

The sensitivity indices for each parameter in the tuberculosis sub-model (7) with respect to R_{0_T} is computed by using the equation (9), and the corresponding sensitivity indices are shown in Figure 3.

The sensitivity analysis of the tuberculosis sub-model revealed that the tuberculosis transmission rate β_t, and the recruitment rate ω have a high positive impact on the spread of the virus. The analysis suggests that the magnitude of the impacts of β_t and ω on the spread of COVID-19 are the same because the number of secondary infections increases when the value of these parameters also increases [22]. Also, the progression rate of tuberculosis from asymptomatic to symptomatic r_t has a positive impact on the spread of COVID-19 virus. In contrast, the parameters δ_t, μ, and μ_2 have a negative impact, which means that increasing the value of such parameters will decrease the number of people infected with tuberculosis.

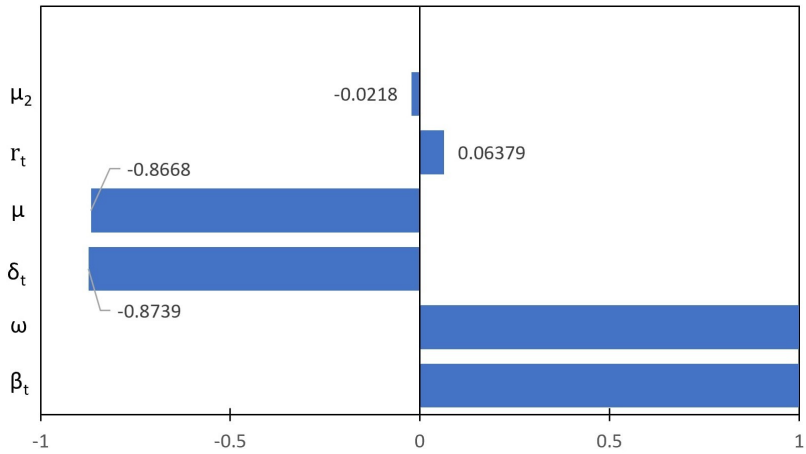

Figure 3: Sensitivity indices of the tuberculosis sub-model parameters

3.7. COVID-19 and Tuberculosis Co-infection Model

In this subsection, we examine the transmission dynamics of the co-infection model for COVID-19 and tuberculosis which is described by system (1). When the environment is free from both diseases, the system reaches the disease-free equilibrium $E_{0_{CT}}$ and is given by

$$E_{0_{CT}} = (S, E_C, I_C, Q_C, E_{CT}, I_{CT}, Q_{CT}, E_T, I_T, Q_T) = \Big(\frac{\omega}{\mu}, 0, 0, 0, 0, 0, 0, 0, 0, 0\Big).$$

The basic reproduction number of the co-infection model is governed by the COVID-19 and tuberculosis sub-models, with the dominant value determining the overall transmission dynamics. Utilizing the Next Generation Matrix (NGM) approach, we compute the basic reproduction number of the co-infection model, where the transmission matrix $\mathcal{F}$ and transition matrix $\mathcal{V}$ are given by

$$\mathcal{F} = \begin{pmatrix} \beta_c(E_C + I_C)S \\ 0 \\ 0 \\ 0 \\ 0 \\ 0 \\ \beta_t I_T S \\ 0 \\ 0 \end{pmatrix} \quad \text{and} \quad \mathcal{V} = \begin{pmatrix} \alpha_t\beta_t I_T E_C + (r_c + \delta_e + \mu)E_C \\ -r_c E_C + (\delta_c + \mu + \mu_1)I_C \\ -\delta_e E_C - \delta_c I_C - \gamma_{ct} Q_{CT} + (\gamma_c + \mu + \mu_4)Q_C \\ -\alpha_t\beta_t I_T E_C - \alpha_c\beta_c(E_C + I_C)E_T + (r_{ct} + \mu)E_{CT} \\ -r_{ct} E_{CT} + (\delta_{ct} + \mu + \mu_3)I_{CT} \\ -\delta_{ct} I_{CT} + (\gamma_{tc} + \gamma_{ct} + \mu + \mu_6)Q_{CT} \\ \alpha_c\beta_c(E_C + I_C)E_T + (r_t + \mu)E_T \\ -r_t E_T + (\delta_t + \mu + \mu_2)I_T \\ -\delta_t I_T - \gamma_{tc} Q_{CT} + (\gamma_t + \mu + \mu_5)Q_T \end{pmatrix}.$$

Accordingly, the Jacobian matrices of $\mathcal{F}$ and $\mathcal{V}$ evaluated at the disease-free equilibrium point $E_{0_{CT}}$ are

$$F = \begin{pmatrix} \frac{\beta_c\omega}{\mu} & \frac{\beta_c\omega}{\mu} & 0 & 0 & 0 & 0 & 0 & 0 & 0 \\ 0 & 0 & 0 & 0 & 0 & 0 & 0 & 0 & 0 \\ 0 & 0 & 0 & 0 & 0 & 0 & 0 & 0 & 0 \\ 0 & 0 & 0 & 0 & 0 & 0 & 0 & 0 & 0 \\ 0 & 0 & 0 & 0 & 0 & 0 & 0 & 0 & 0 \\ 0 & 0 & 0 & 0 & 0 & 0 & 0 & 0 & 0 \\ 0 & 0 & 0 & 0 & 0 & 0 & 0 & \frac{\beta_t\omega}{\mu} & 0 \\ 0 & 0 & 0 & 0 & 0 & 0 & 0 & 0 & 0 \\ 0 & 0 & 0 & 0 & 0 & 0 & 0 & 0 & 0 \end{pmatrix} \text{ and}$$

$$V = \begin{pmatrix} A_1 & 0 & 0 & 0 & 0 & 0 & 0 & 0 & 0 \\ -r_c & A_2 & 0 & 0 & 0 & 0 & 0 & 0 & 0 \\ -\epsilon_C & -\rho_C & A_3 & 0 & 0 & -\gamma_{ct} & 0 & 0 & 0 \\ 0 & 0 & 0 & C_1 & 0 & 0 & 0 & 0 & 0 \\ 0 & 0 & 0 & -r_{ct} & C_2 & 0 & 0 & 0 & 0 \\ 0 & 0 & 0 & 0 & -\delta_{ct} & C_3 & 0 & 0 & 0 \\ 0 & 0 & 0 & 0 & 0 & 0 & B_1 & 0 & 0 \\ 0 & 0 & 0 & 0 & 0 & 0 & -\theta_{_T} & B_2 & 0 \\ 0 & 0 & 0 & 0 & 0 & -\gamma_{tc} & 0 & -\rho_{_T} & B_3 \end{pmatrix},$$

respectively, where

$$C_1 = r_{ct} + \mu, C_2 = \delta_{ct} + \mu + \mu_3, \text{ and } C_3 = \gamma_{tc} + \gamma_{ct} + \mu + \mu_5. \tag{10}$$

Hence,

$$FV^{-1} = \begin{pmatrix} \frac{\beta_c\omega}{\mu A_1} + \frac{\beta_c\omega r_c}{\mu A_1 A_2} & \frac{\beta_c\omega}{\mu A_2} & 0 & 0 & 0 & 0 & 0 & 0 & 0 \\ 0 & 0 & 0 & 0 & 0 & 0 & 0 & 0 & 0 \\ 0 & 0 & 0 & 0 & 0 & 0 & 0 & 0 & 0 \\ 0 & 0 & 0 & 0 & 0 & 0 & 0 & 0 & 0 \\ 0 & 0 & 0 & 0 & 0 & 0 & 0 & 0 & 0 \\ 0 & 0 & 0 & 0 & 0 & 0 & 0 & 0 & 0 \\ 0 & 0 & 0 & 0 & 0 & 0 & \frac{\beta_t\omega r_t}{\mu B_1 B_2} & \frac{\beta_t\omega}{\mu B_2} & 0 \\ 0 & 0 & 0 & 0 & 0 & 0 & 0 & 0 & 0 \\ 0 & 0 & 0 & 0 & 0 & 0 & 0 & 0 & 0 \end{pmatrix}$$

Consequently, the nonzero eigenvalues are

$$\frac{\beta_c\omega(\delta_c + \mu + \mu_1 + r_c)}{\mu(r_c + \delta_e + \mu)(\delta_c + \mu + \mu_1)} \text{ and } \frac{\beta_t\omega r_t}{\mu(r_t + \mu)(\delta_t + \mu + \mu_2)}.$$

Thus, the basic reproduction number of the COVID-19 and tuberculosis co-infection model (1) is

$$R_{0_{CT}} = max\left\{\frac{\beta_c\omega(\delta_c + \mu + \mu_1 + r_c)}{\mu(r_c + \delta_e + \mu)(\delta_c + \mu + \mu_1)}, \frac{\beta_t\omega r_t}{\mu(r_t + \mu)(\delta_t + \mu + \mu_2)}\right\}.$$

3.8. Stability Analysis for the Co-infection Model of COVID-19 and Tuberculosis

Theorem 9. *If $R_{0_{CT}} < 1$, then the co-infection system (1) is locally asymptotically stable at the disease-free equilibrium point $E_{0_{CT}}$ and unstable otherwise.*

Proof. The Jacobian matrix of system (1) evaluated at DFE $E_{0_{CT}}$ is

$$J_{E_{0_{CT}}} = \begin{pmatrix} -\mu & \frac{-\beta_c\omega}{\mu} & \frac{-\beta_c\omega}{\mu} & 0 & 0 & 0 & 0 & 0 & \frac{-\beta_t\omega}{\mu} & 0 \\ 0 & \frac{\beta_c\omega}{\mu} - A_1 & \frac{\beta_c\omega}{\mu} & 0 & 0 & 0 & 0 & 0 & 0 & 0 \\ 0 & r_c & -A_2 & 0 & 0 & 0 & 0 & 0 & 0 & 0 \\ 0 & \delta_e & \delta_c & -A_3 & 0 & 0 & \gamma_{ct} & 0 & 0 & 0 \\ 0 & 0 & 0 & 0 & -C_1 & 0 & 0 & 0 & 0 & 0 \\ 0 & 0 & 0 & 0 & r_{ct} & -C_2 & 0 & 0 & 0 & 0 \\ 0 & 0 & 0 & 0 & 0 & \delta_{ct} & -C_3 & 0 & 0 & 0 \\ 0 & 0 & 0 & 0 & 0 & 0 & 0 & -B_1 & \frac{\beta_t\omega}{\mu} & 0 \\ 0 & 0 & 0 & 0 & 0 & 0 & 0 & r_t & -B_2 & 0 \\ 0 & 0 & 0 & 0 & 0 & 0 & \gamma_{tc} & 0 & \delta_t & -B_3 \end{pmatrix}$$

Then the linear factors of the characteristic polynomial of $J_{E_{0_{CT}}}$ are

$$(-\mu-\lambda), (-B_3-\lambda), (-A_3-\lambda), (-C_3-\lambda), (-C_2-\lambda), (-C_1-\lambda)$$

and the second order polynomial factors are

$$\lambda^2 + (B_1+B_2)\lambda + B_1B_2 - \frac{\beta_c\omega r_t}{\mu} \quad \text{and} \quad \lambda^2 + \Big(A_1 + A_2 - \frac{\beta_c\omega}{\mu}\Big)\lambda + A_1A_2 - \frac{\beta_c\omega A_2}{\mu} - \frac{\beta_c\omega r_c}{\mu}.$$

Similar to the proofs of Theorem (1) and Theorem (6), we can see that the second order polynomials above have roots with negative real parts. Therefore, the co-infection system (1) of COVID-19 and tuberculosis is locally asymptotically stable at the disease-free equilibrium point $E_{0_{CT}}$ when $R_{0_{CT}} < 1$ and unstable otherwise.

To examine the global stability of the co-infection model (1) at the disease-free equilibrium $E_{0_{CT}}$, we employ the method developed by Castillo-Chavez [7]. Rewriting the co-infection model (1) as

$$\begin{cases} \dfrac{dX}{dt} = F(X,Z) \\ \dfrac{dZ}{dt} = G(X,Z), \end{cases}$$

where $X = S$ and $Z = (E_C, I_C, Q_C, E_{CT}, I_{CT}, Q_{CT}, E_T, I_T, Q_T)$ denote the noninfectious and infectious states, respectively. The disease-free equilibrium is denoted now as

$$E_{0_{CT}} = (X_0, 0) \ \text{ where } \ X_0 = \frac{\omega}{\mu}.$$

The conditions stated below are necessary to ensure the global asymptotic stability of $E_{0_{CT}}$ for $R_{0_{CT}} < 1$:

(i) For $\frac{dX}{dt} = F(X,0)$, X_0 is globally asymptotically stable

(ii) $G(X,Z) = AZ - \hat{G}(X,Z)$, $\hat{G}(X,Z) \geq 0$, for $(X,Z) \in \omega$ where $A = D_Z G(E_{0_{CT}}, 0)$ is a Metzler matrix (the non-diagonal entities of A are non-negative), and ω is the biological feasible region of the model.

From the co-infection model (1), we have

$$\frac{dX}{dt} = F(X,Z) = \omega - \beta_c(E_C + I_C) - \beta_t I_T S - \mu S.$$

Hence,

$$\frac{dX}{dt} = F(X,0) = \omega - \mu S \quad \text{and} \quad X_0 \ \text{ is globally asymptotically stable.}$$

Moreover,

$$\frac{dZ}{dt} = G(X,Z) = \begin{pmatrix} \beta_c(E_C+I_C)S - \alpha_t\beta_t I_T E_C - (r_c+\delta_e+\mu)E_C \\ r_c E_C - (\delta_c+\mu+\mu_1)I_C \\ \delta_e E_C + \delta_c I_C + \gamma_{ct} Q_{CT} - (\gamma_c+\mu+\mu_4)Q_C \\ \alpha_t\beta_t I_T E_C + \alpha_c\beta_c(E_C+I_C)E_T - (r_{ct}+\mu)E_{CT} \\ r_{ct}E_{CT} - (\delta_{ct}+\mu+\mu_3)I_{CT} \\ \delta_{ct} I_{CT} - (\gamma_{tc}+\gamma_{ct}+\mu+\mu_6)Q_{CT} \\ \beta_t I_T S - \alpha_c\beta_c(E_C+I_C)E_T - (r_t+\mu)E_T \\ r_t E_T - (\delta_t+\mu+\mu_2)I_T \\ \delta_t I_T + \gamma_{tc} Q_{CT} - (\gamma_t+\mu+\mu_5)Q_T \end{pmatrix}$$

Consequently,

$$A = \begin{pmatrix} \frac{\beta_c\omega}{\mu} - A_1 & \frac{\beta_c\omega}{\mu} & 0 & 0 & 0 & 0 & 0 & 0 & 0 \\ r_c & -A_2 & 0 & 0 & 0 & 0 & 0 & 0 & 0 \\ \delta_e & \delta_c & -A_3 & 0 & 0 & \gamma_{ct} & 0 & 0 & 0 \\ 0 & 0 & 0 & -C_1 & 0 & 0 & 0 & 0 & 0 \\ 0 & 0 & 0 & r_{ct} & -C_2 & 0 & 0 & 0 & 0 \\ 0 & 0 & 0 & 0 & \delta_{ct} & -C_3 & 0 & 0 & 0 \\ 0 & 0 & 0 & 0 & 0 & 0 & -B_1 & \frac{\beta_t\omega}{\mu} & 0 \\ 0 & 0 & 0 & 0 & 0 & 0 & r_t & -B_2 & 0 \\ 0 & 0 & 0 & 0 & 0 & \gamma_{tc} & 0 & \delta_t & -B_3 \end{pmatrix}.$$

where $A_i, B_i, C_i, i = 1,2,3$ are given in equations 5, 8, and 10, respectively. Then,

$$AZ = \begin{pmatrix} \left(\frac{\beta_c\omega}{\mu} - A_1\right)E_C + \frac{\beta_c\omega}{\mu} I_C \\ r_c E_C - A_2 I_C \\ \delta_e E_C + \delta_c I_C - A_3 Q_C + \gamma_{ct} Q_{CT} \\ -C_1 E_{CT} \\ r_{ct} E_{CT} - C_2 I_{CT} \\ \delta_{ct} I_{CT} - C_3 Q_{CT} \\ -B_1 E_T + \frac{\beta_t\omega}{\mu} I_T \\ r_t E_T - B_2 I_T \\ \gamma_{tc} Q_{CT} + \delta_t I_T - B_3 Q_T \end{pmatrix}.$$

In effect,

$$\hat{G}(X,Y) = \begin{pmatrix} \hat{G}_1(X,Y) \\ \hat{G}_2(X,Y) \\ \hat{G}_3(X,Y) \\ \hat{G}_4(X,Y) \\ \hat{G}_5(X,Y) \\ \hat{G}_6(X,Y) \\ \hat{G}_7(X,Y) \\ \hat{G}_8(X,Y) \\ \hat{G}_9(X,Y) \end{pmatrix} = \begin{pmatrix} \frac{\beta_c\omega}{\mu}(E_C+I_C) - \beta_c(E_C+I_C)S + \alpha_t\beta_t I_T E_C \\ 0 \\ 0 \\ -\alpha_t\beta_t E_C - \alpha_c\beta_c(E_C+I_C)E_T \\ 0 \\ 0 \\ \alpha_c\beta_c(E_C+I_c)E_T \\ 0 \\ 0 \end{pmatrix}.$$

Observe that $\hat{G}_5(X,Y) = -\alpha_t\beta_t E_C - \alpha_c\beta_c(E_C + I_C)E_T < 0$, which means that the condition 2 is not satisfied. Therefore, the co-infection model may not be globally asymptotically stable at the disease-free equilibrium $E_{0_{CT}}$.

4. Simulation

In the preceding sections, we examined the stability behaviors of the sub-models (2) and (7), as well as the co-infection model (1). In this section, we present numerical simulations to illustrate the theoretical findings. The parameter values utilized in these simulations are provided in Table 1.

4.1. Numerical Simulation of the COViD-19 Sub-model

Simulation 1. The given parameter values are based on Table 1, $\omega = 3$, $\delta_e = 0.74$, and $\delta_c = 0.78$. Subsequently, we obtain $R_{0_C} = 0.9922$ and the disease-free equilibrium is $E_{0_C} = (63, 0, 0, 0)$. We take the following initial conditions of the compartments of the COVID-19 sub-model: a. (100,70,45,35), b. (80,135,105,47), c. (75,87,38,52), and d. (240,87,213,97). Figure 4 shows that for different initial conditions, the lines of the solutions converge to $E_{0_C} = (63, 0, 0, 0)$. It implies that the COVID-19 sub-model is locally asymptotically stable at the disease-free equilibrium when $R_{0_C} < 1$.

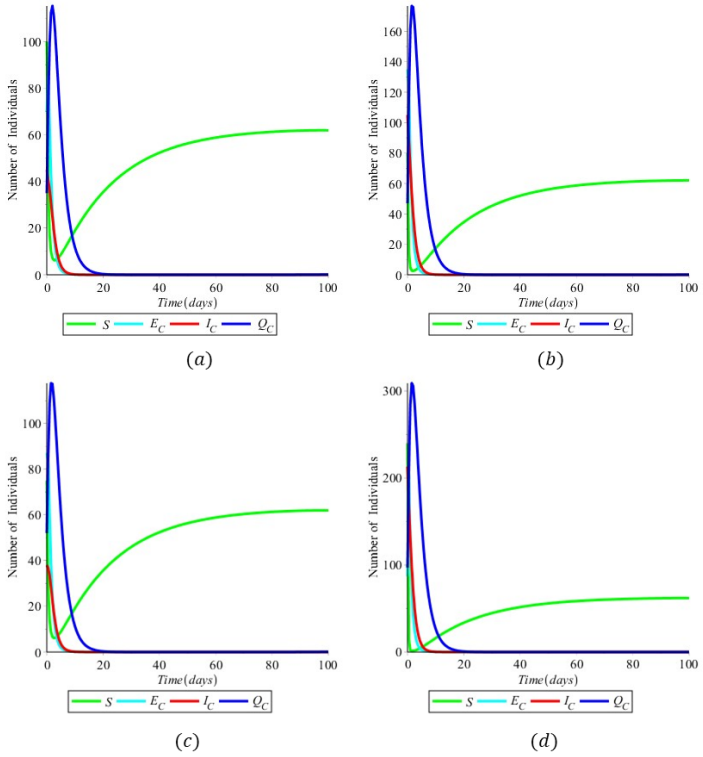

Figure 4: (Simulation 1) The COVID-19 sub-model is locally asymptotically stable at E_{0_C} when $R_{0_C} < 1$.

Simulation 2. Consider the same parameter values as in Simulation 1, except for the decreased values of $\delta_e = 0.24$ and $\delta_c = 0.31$. As a result, R_{0_C} becomes 4.0117, and the disease-free equilibrium remains unchanged at $E_{0_C} = (63, 0, 0, 0)$. By using the same initial conditions as in Simulation 1, we observe from Figure 5 that the lines of the solutions do not converge to $E_{0_C} = (63, 0, 0, 0)$. This indicates that the COVID-19 sub-model is unstable at the disease-free equilibrium when $R_{0_C} > 1$. Moreover, since we have obtained $R_{0_C} = 4.0117$ and the endemic equilibrium point $E_{1_C} = (23, 4, 3, 5)$ now exists, we can observe that the lines of the solutions converge to $E_{1_C} = (23, 4, 3, 5)$. Therefore, the COVID-19 sub-model is locally asymptotically stable at the endemic point whenever $R_{0_C} > 1$.

Figures 4 and 5 illustrate the effect of quarantine measures in the COVID-19 sub-model (2). The findings indicate that when the intensity of quarantine measures is low, exposed and infected individuals with COVID-19 continue to transmit the disease to susceptible individuals. As a result, the number of exposed and infected cases increases. As observed in Figure 4, the number of susceptible individuals remains higher than that of exposed and infected individuals when the quarantine measure is stringent, suggesting that quarantine measures effectively reduce the spread of infection. Furthermore, Figure 4 shows that the number of exposed and infected individuals approaches zero, indicating widespread compliance with quarantine protocols. Consequently, the disease will eventually be eradicated within the community over time.

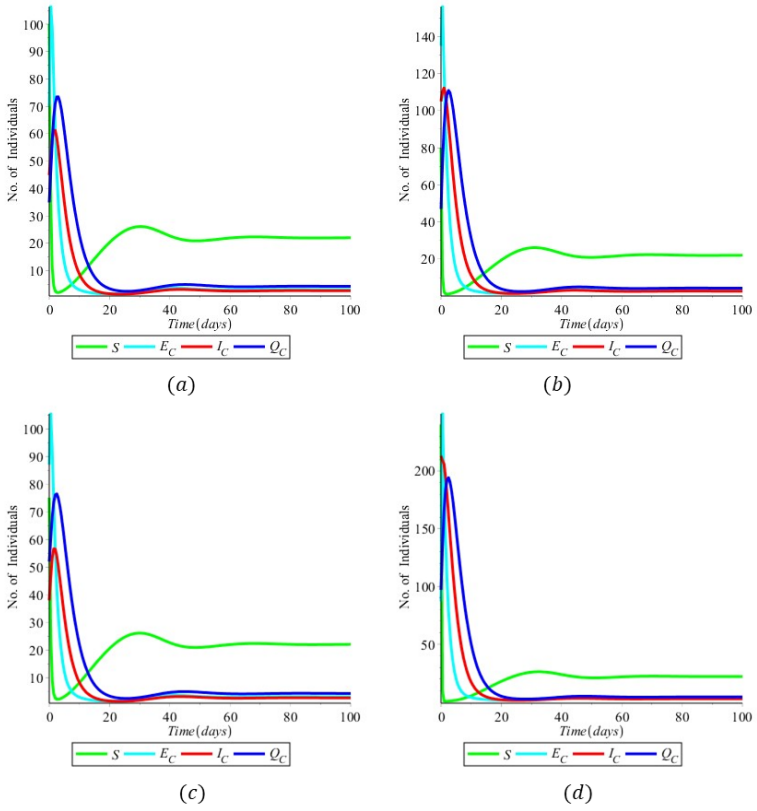

Figure 5: (Simulation 2) The COVID-19 sub-model is locally asymptotically stable at E_{1_C} when $R_{0_C} > 1$.

4.2. Numerical Simulation for Tuberculosis Sub-model

Simulation 3. The given parameter values are based on Table 1, $\omega = 4$ and $\delta_t = 0.95$. Subsequently, we obtain $R_{0_T} = 0.9349$ and the disease-free equilibrium is $E_{0_T} = (84, 0, 0, 0)$. To support our result, we take the following initial conditions: (a). (50,90,27,53), (b). (150,34,67,93), (c). (60,200,87,52) and (d). (230,47,129,109). Figure 6 shows that for different initial conditions, the lines of the solutions converge to $E_{0_T} = (84, 0, 0, 0)$. It means that the tuberculosis sub-model (7) is locally asymptotically stable at the disease-free equilibrium when $R_{0_T} < 1$.

Simulation 4. Consider the same parameter values as in Simulation 3, except for the decreased value of $\delta_t = 0.21$. As a result, $R_{0_T} = 3.5192$ and the disease-free equilibrium remains unchanged at $E_{0_T} = (84, 0, 0, 0)$. We observe from Figure 7 that the lines of the solutions do not converge to $E_{0_T} = (84, 0, 0, 0)$. This indicates that the tuberculosis sub-model is unstable at the disease-free equilibrium when $R_{0_T} > 1$. Furthermore, since we have obtained $R_{0_T} = 3.5192$ and the endemic equilibrium point $E_{1_T} = (23, 4, 11, 9)$ now exists, we can observe that the lines of the solutions converge to $E_{1_T}(23, 4, 11, 9)$. Therefore, the tuberculosis sub-model is locally asymptotically stable at the endemic equilibrium point whenever $R_{0_T} > 1$.

Figures 6 and 7 illustrate the effect of quarantine measures in the tuberculosis sub-model (7). The results are similar to those of the COVID-19 sub-model. When the value of the quarantine measure is low, infected individuals continue transmitting the disease, leading to an increase in cases. Conversely, a high quarantine measure helps control the spread of tuberculosis, ultimately leading to its eradication over time.

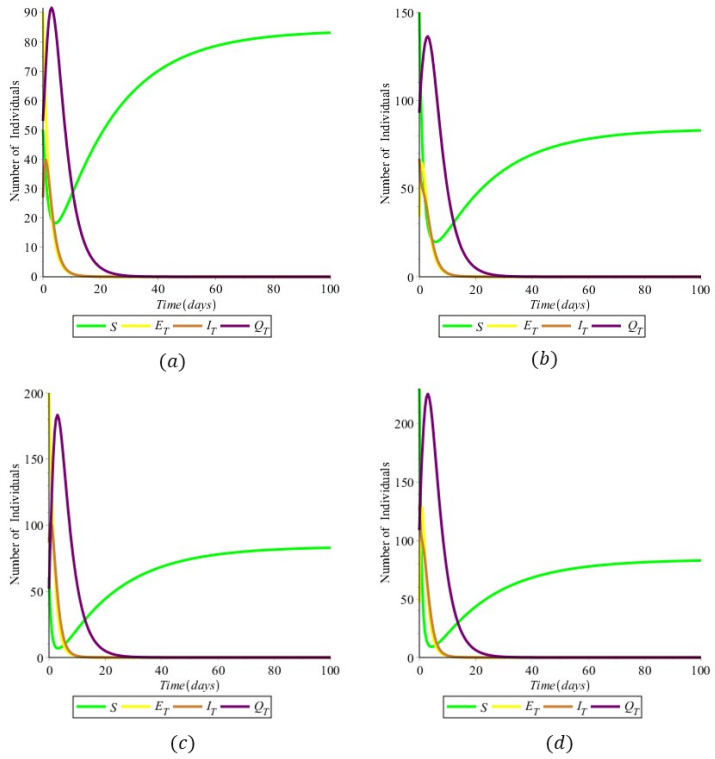

Figure 6: (Simulation 3) The TB sub-model is locally asymptotically stable at E_{0_T} when $R_{0_T} < 1$.

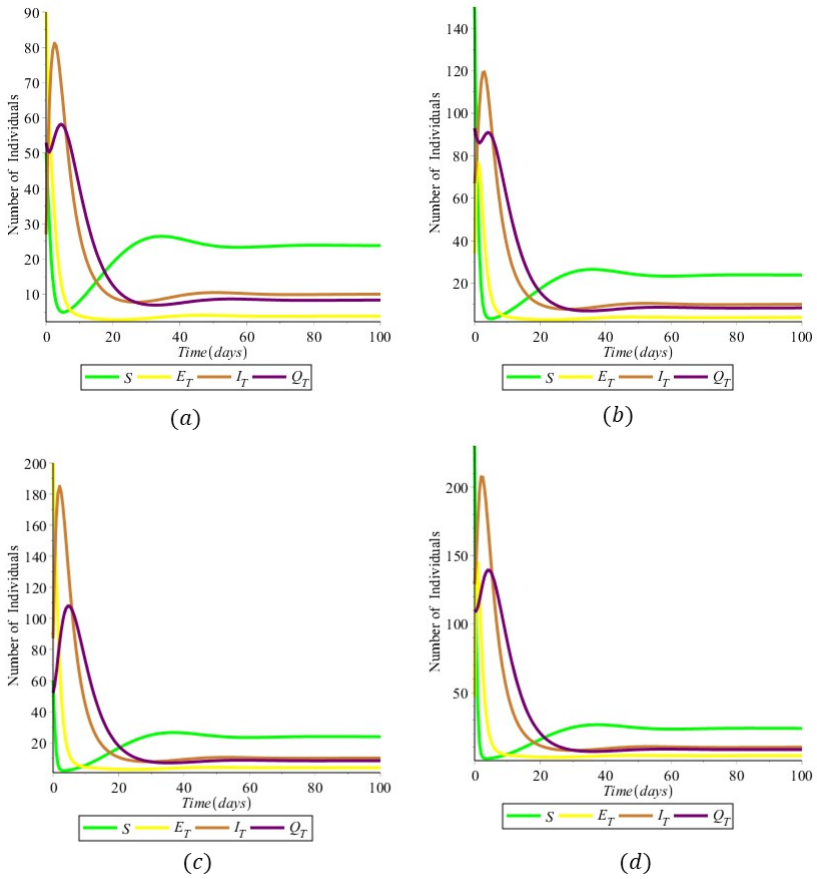

Figure 7: (Simulation 4) The TB sub-model is locally asymptotically stable at E_{1_T} when $R_{0_T} > 1$.

4.3. Numerical Simulation for Co-infection Model

Simulation 5. The given parameter values are based on Table 1, $\omega = 2$ and $\delta_e = 0.57$, $\delta_c = 0.61$, and $\delta_t = 0.46$. Subsequently, we obtain $R_{0_C} = 0.9749$ and $R_{0_T} = 0.9099$ and the disease-free equilibrium is $(42, 0, 0, 0, 0, 0, 0, 0, 0, 0)$. Hence, the basic reproduction number of the co-infection model (1) is $R_{0_C} = 0.9749$. We take the following initial conditions: a. (100,45,30,0,35,25,0,35,20,0), b.(100,55,64,10,45,35,10,70,40,5), c.(150,100,78,70,48,37,10,64,28,19), d.(300,10,20,0,10,9,0,15,15,0). Figure 8 shows that the lines of the solutions converge to $(42, 0, 0, 0, 0, 0, 0, 0, 0, 0)$. This indicates that the co-infection model (1) is locally asymptotically stable at the disease-free equilibrium when $R_{0_{CT}} < 1$.

Simulation 6. Consider the same parameter values as in Simulation 5, except for the decreased value of $\delta_e = 0.02$, $\delta_c = 0.05$ and $\delta_t = 0.06$. As a result, $R_{0_C} = 13.1021$ and $R_{0_T} = 4.0021$ and the disease-free equilibrium remains unchanged at $(42, 0, 0, 0, 0, 0, 0, 0, 0, 0)$. We observe from Figure 9 that the lines of the solutions do not converge to $(42, 0, 0, 0, 0, 0, 0, 0, 0, 0)$. This indicates that the co-infection model is unstable at the disease-free equilibrium when $R_{0_{CT}} > 1$.

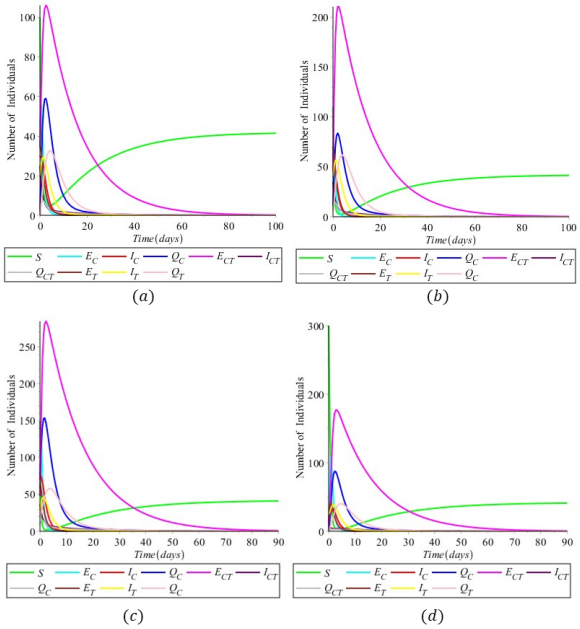

Figure 8: (Simulation 5) The Co-infection model is locally asymptotically stable at the disease-free equilibrium when $R_{0_{CT}} < 1$

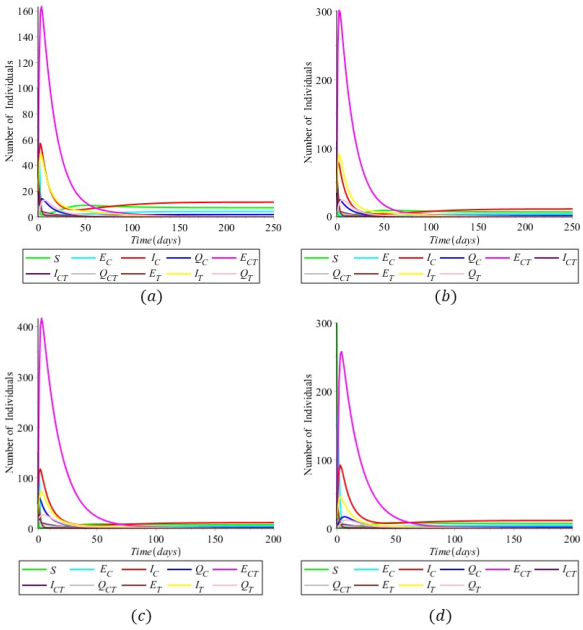

Figure 9: (Simulation 6) The Co-infection model is locally asymptotically stable at the disease-free equilibrium when $R_{0_{CT}} < 1$

5. Conclusion

In this paper, a deterministic mathematical model for the co-infection of COVID-19 and tuberculosis, incorporating quarantine measures, is proposed and analyzed. It is demonstrated that the solutions of the COVID-19 and tuberculosis sub-models are unique, positive, and bounded. The equilibrium points and basic reproduction numbers of both the sub-models and the co-infection model were computed independently. Subsequently, it is shown that both sub-models exhibit locally and globally asymptotically stable at the disease-free equilibrium when the basic reproduction number is less than 1, and unstable otherwise. Additionally, the endemic equilibrium is locally asymptotically stable when the basic reproduction number exceeds 1. Moreover, the co-infection model is locally and globally asymptotically stable at the disease-free equilibrium when the maximum reproduction number of the sub-models is less than 1. To further support and illustrate these analytical findings, multiple numerical simulations were conducted. The results of these simulations indicate that quarantine measures effectively mitigate the spread of both diseases.

Based on the model results, public health initiatives should prioritize the strengthening of quarantine measures for individuals infected with COVID-19, tuberculosis, or both. Quarantine interventions effectively reduce the basic reproduction number below unity, thereby demonstrating their critical role as a fundamental public health strategy for controlling current co-infection outbreaks. Furthermore, integrating quarantine protocols could significantly enhance disease mitigation and may ultimately lead to the eradication of COVID-19 and tuberculosis co-infections.

This study assumes a homogeneous population structure without accounting for differences in age, immunity levels, or social behavior, which may affect disease transmission dynamics in real-world settings. Additionally, the model does not explicitly incorporate vaccination strategies or their effects, such as vaccine efficacy, coverage, or waning immunity, which are critical factors in controlling COVID-19 and tuberculosis co-infections. Future work could extend the current model to include population heterogeneity, vaccination and reinfection dynamics to provide a more comprehensive assessment of intervention strategies.

Conflict of Interest

The authors declare no conflicts interest.

Acknowledgements

The authors would like to thank everyone who supported and contributed to this study. Special thanks to our colleagues for their valuable insights, constructive feedback, and continued support throughout the research process.

References

[1] Appiah, R. F., Jin, Z., Yang, J., Asamoah, J. K. K., & Wen, Y. (2024). Mathematical modeling of two strains tuberculosis and COVID-19 vaccination model: A co-infection study with cost-effectiveness analysis. Frontiers in Applied Mathematics and Statistics, 10, 1373565. https://doi.org/10.3389/fams.2024.1373565

[2] Bandekar, S. R., & Ghosh, M. (2022). A co-infection model on TB - COVID-19 with optimal control and sensitivity analysis. Mathematics and Computers in Simulation, 200, 1–31. https://doi.org/10.1016/j.matcom.2022.04.001

[3] Bernstein, D., & Bhat, S. (1999). Nonnegativity, reducibility, and semistability of mass action kinetics. Proceedings of the 38th IEEE Conference on Decision and Control (Cat. No.99CH36304). https://doi.org/10.1109/cdc.1999.831248
[4] Birkhoff G, Rota GC. Ordinary differential equations. 4th ed.. New York: John Wiley and Sons Inc; 1989.
[5] Boudaoui, A., Moussa, Y. E. H., Hammouch, Z., & Ullah, S. (2021). A fractional-order model describing the dynamics of the novel coronavirus (COVID-19) with nonsingular kernel. Chaos, Solitons & Fractals, 146, Article 110859. https://doi.org/10.1016/j.chaos.2021.110859
[6] Bronson, R. (1994). Schaum's Outline of Theory and Problems of Differential Equations. McGraw Hill Professional.
[7] Castillo-Chavez, C., Feng, Z., & Huang, W. (2002). On the computation of R0 and its role on global stability. Mathematical Approaches for Emerging and Reemerging Infectious Diseases: An Introduction, 229-250. https://doi.org/10.1007/978-1-4757-3667-0_13
[8] Coronavirus disease (COVID-19) pandemic. (2023, May 24). https://www.who.int/europe/emergencies/situations/covid-19
[9] Chen, Y., Wang, Y., Fleming, J. & et al. Active or latent tuberculosis increases susceptibility to COVID-19 and disease severity
[10] COVID-19 and Your Health. (2020, February 11). Centers for Disease Control and Prevention. https://www.cdc.gov/coronavirus/2019-ncov/your-health/about-covid-19.html
[11] Diabaté, A. B., Sangaré, B., & Koutou, O. (2024). Optimal control analysis of a COVID-19 and Tuberculosis (TB) co-infection model with an imperfect vaccine for COVID-19. SeMA Journal, 81, 429–456. https://doi.org/10.1007/s40324-023-00330-8
[12] Diekmann O, Heesterbeek JA, Roberts MG. The construction of next-generation matrices for compartmental epidemic models. J R Soc Interface. 2010 Jun 6;7(47):873-85. doi: 10.1098/rsif.2009.0386. Epub 2009 Nov 5. PMID: 19892718; PMCID: PMC2871801.
[13] Fahlena, H., Oktaviana, W. R., Farida, F., Sudirman, S., Nuraini, N., & Soewono, E. (2021). Analysis of A Coendemic Model of COVID-19 and Dengue Disease. Communication in Biomathematical Sciences, 4(2), 138–151. https://doi.org/10.5614/cbms.2021.4.2.5
[14] Goudiaby, M. S., Gning, L., Diagne, M., Dia, B. M., Rwezaura, H., & Tchuenche, J. M. (2022). Optimal control analysis of a COVID-19 and tuberculosis co-dynamics model. Informatics in Medicine Unlocked, 28, 100849. https://doi.org/10.1016/j.imu.2022.100849
[15] Hamou, A. A., Rasul, R. R. Q., Hammouch, Z., & Özdemir, N. (2022). Analysis and dynamics of a mathematical model to predict unreported cases of COVID-19 epidemic in Moroco. Computational and Applied Mathematics, 41(1), 289. https://doi.org/10.1007/s40314-022-01990-4
[16] Hutson V, Schmitt K. Permanence and the dynamics of biological systems. Math Biosci 1992;111:1–71.
[17] Inayaturohmat, F., Anggriani, N., & Supriatna, A. K. (2022). A mathematical model of tuberculosis and COVID-19 coinfection with the effect of isolation and treatment. Frontiers in Applied Mathematics and Statistics, 8. https://doi.org/10.3389/fams.2022.958081
[18] Khan, M. S., Atangana, A., Alzahrani, E. O., & Fatmawati. (2020). The dynamics of COVID-19 with quarantined and isolation. Advances in Difference Equations, 2020(1). https://doi.org/10.1186/s13662-020-02882-9
[19] Khurana, A.K., Aggarwal, D. The (in)significance of TB and COVID-19 co-infection, Eur. Respir. J. 56(2) (2020) 2002105.
[20] Mallah SI, Ghorab OK, Al-Salmi S, Abdellatif OS, Tharmaratnam T, Iskandar MA, Sefen JAN, Sidhu P, Atallah B, El-Lababidi R, Al-Qahtani M. COVID-19: breaking down a global health crisis. Ann Clin Microbiol Antimicrob. 2021 May 18;20(1):35. doi: 10.1186/s12941-021-00438-7. PMID: 34006330; PMCID: PMC8129964.

[21] Margalit, D. & Rabinoff, J. (2022). Interactive Linear Algebra. Mathematics LibreTexts. https://math.libretexts.org/Bookshelves/Linear Algebra/Interactive Linear Algebra (Margalit and Rabinoff)
[22] Martcheva, M. (2015). An Introduction to Mathematical Epidemiology, vol.61, Springer.
[23] Mekonen, K. G., Balcha, S. F., Obsu, L. L., & Hassen, A. A. (2022). Mathematical Modeling and Analysis of TB and COVID-19 Coinfection. Journal of Applied Mathematics, 2022, 1–20. https://doi.org/10.1155/2022/2449710
[24] Mekonen, K. G., & Obsu, L. L. (2022). Mathematical modeling and analysis for the co-infection of COVID-19 and tuberculosis. Heliyon, 8(10), e11195. https://doi.org/10.1016/j.heliyon.2022.e11195
[25] McQuaid, C., Vassall, A., Cohen, T., & et al. The impact of COVID-19 on TB: a review of the data. The International Journal of Tuberculosis and Lung Disease, vol. 25, no. 6, pp. 436–446, 2021.
[26] Ojo, M. M., Nyabadza, F., & Adamu, M. O. (2023). A mathematical model for the co-dynamics of COVID-19 and tuberculosis. Journal of Applied Mathematics and Computing, 71, 893–916. https://doi.org/10.1007/s12190-022-01611-4
[27] Ojo, M. M., Peter, O. J., Goufo, E. F. D., & Nisar, K. S. (2023). A mathematical model for the co-dynamics of COVID-19 and tuberculosis. Mathematics and Computers in Simulation, 207, 499–520. https://doi.org/10.1016/j.matcom.2023.01.014
[28] Omame, A., Rwezaura, H., Diagne, M., Inyama, S. C., & Tchuenche, J. M. (2021). COVID-19 and dengue co-infection in Brazil: optimal control and cost-effectiveness analysis. European Physical Journal Plus, 136(10). https://doi.org/10.1140/epjp/s13360-021-02030-6
[29] Perko, L. (2001). Differential equations and dynamical systems (3rd ed.). Springer-Verlag, New York, Inc.
[30] Philippines: WHO Coronavirus Disease (COVID-19) Dashboard With Vaccination Data. (n.d.). WHO Coronavirus (COVID-19) Dashboard With Vaccination Data. https://covid19.who.int/region/wpro/country/ph
[31] Ringa, N., Diagne, M., Rwezaura, H., Omame, A., Tchoumi, S. Y., & Tchuenche, J. M. (2022). HIV and COVID-19 co-infection: A mathematical model and optimal control. Informatics in Medicine Unlocked, 31, 100978. https://doi.org/10.1016/j.imu.2022.100978
[32] Roskilly, T., & Mikalsen, R. (2015). Chapter Five - Closed-Loop Stability. In Marine systems identification, modeling and control. Butterworth-Heinemann.
[33] Rwezaura, H., Kateta, M., Tchoumi, J. M. N., & Luboobi, L. S. (2022). Mathematical modeling and optimal control of SARS-CoV-2 and tuberculosis co-infection: A case study of Indonesia. AIMS Public Health, 9(3), 420–441. https://doi.org/10.1007/s40808-022-01430-6
[34] Singh, R., Rehman, A. U., Ahmed, T., Ahmad, K., Mahajan, S., Pandit, A. K., Abualigah, L., & Gandomi, A. H. (2023). Mathematical modelling and analysis of COVID-19 and tuberculosis transmission dynamics. Informatics in Medicine Unlocked, 101235. https://doi.org/10.1016/j.imu.2023.101235
[35] T. G. Fund, Global fund results report reveals Covid-19 devastating impact on hiv, tb and malaria programs, results report 2021, 08 September 2021, Tech. rep., The Global Fund, 2021.
[36] Tuberculosis (TB). (2023, April 21). Tuberculosis. https://www.who.int/news-room/fact-sheets/detail/tuberculosis
Manila University, Unpublish Lecture Notes.
[37] Wiggins, S. (1990). Introduction to applied nonlinear dynamical systems and chaos. Springer
[38] WHO Coronavirus (COVID-19) Dashboard. (n.d.). WHO Coronavirus (COVID-19) Dashboard With Vaccination Data. https://covid19.who.int/
[39] World Health Organization: WHO & World Health Organization: WHO. (2023). Tuberculo-

sis. www.who.int. https://www.who.int/news-room/fact-sheets/detail/tuberculosis
[40] World Health Organization. (2021). Tuberculosis and COVID-19. https://www.who.int/teams/global-tuberculosis-programme/covid-19
[41] World Population Review. (n.d.). TB Rate by Country / Tuberculosis Rate by Country 2023. https://worldpopulationreview.com/country-rankings/tb-rate-by-country
[42] Tchoumi, S. Y., Diagne, M., Rwezaura, H., & Tchuenche, J. M. (2021). Malaria and COVID-19 co-dynamics: A mathematical model and optimal control. Applied Mathematical Modelling, 99, 294–327. https://doi.org/10.1016/j.apm.2021.06.016
[43] T.-.G.S. Group, et al., Tuberculosis and COVID 19 co-infection:description of the global cohort, Eur.Respir.J.59(3)(2022). https://doi.org/10.1183/13993003.02538-2021
[44] Van den Driessche P, Watmough J. Reproduction numbers and sub-threshold endemic equilibria for compartmental models of disease transmission. Math Biosci 2002;180(1):29–48.
[45] Vedantu. (n.d.). Diseases- Types of Diseases and Their Symptoms. VEDANTU. https://www.vedantu.com/biology/types-of-diseases-and-symptoms
[46] Zamir, M., Nadeem, F., Abdeljawad, T., & Hammouch, Z. (2021). Threshold condition and non-pharmaceutical interventions' control strategies for elimination of COVID-19. Results in Physics, 20, Article 103698. https://doi.org/10.1016/j.rinp.2020.103698
[47] Zeb, A., Alzahrani, E. O., Erturk, V. S., & Zaman, G. (2020). Mathematical Model for Coronavirus Disease 2019 (COVID-19) Containing Isolation Class. BioMed Research International, 2020, 1–7. https://doi.org/10.1155/2020/3452402